Dissipative spin chains: Implementation with cold atoms and steady-state properties

Heike Schwager,[1] J. Ignacio Cirac,[1] and Géza Giedke[1,2]
[1]*Max-Planck-Institut für Quantenoptik, Hans-Kopfermann–Str. 1, D-85748 Garching, Germany*
[2]*M5, Zentrum Mathematik, TU München, L.-Boltzmannstr. 3, D–85748 Garching, Germany*
(Received 3 August 2012; published 13 February 2013)

We propose a quantum optical implementation of a class of dissipative spin systems, including the XXZ and Ising model, with ultracold atoms in optical lattices. By employing the motional degree of freedom of the atoms and detuned Raman transitions, we show how to obtain engineerable dissipation and a tunable transversal magnetic field, enabling the study of the dynamics and steady-states of dissipative spin models. As an example of effects made accessible this way, we consider small spin chains and weak dissipation and show by numerical simulation that steady-state expectation values display pronounced peaks at certain critical system parameters. We show that this effect is related to degeneracies in the Hamiltonian and derive a sufficient condition for its occurrence.

DOI: 10.1103/PhysRevA.87.022110 PACS number(s): 03.65.Yz, 03.67.Lx

I. INTRODUCTION

Quantum spin models play a fundamental role for the theoretical and experimental study of quantum many-body effects. They represent paradigmatic systems exhibiting, e.g., quantum phase transitions and peculiar forms of matter [1]. They also provide toy models for description of many solid state systems. Ultracold atoms in optical lattices [2] have emerged as a system that is especially suited to study the low-energy sector of quantum spin systems with the promise to eventually simulate theoretical models in large, controlled quantum systems.

To observe these effects, coupling to uncontrolled degrees of freedom has to be kept to a minimum, since it leads to dissipation and decoherence [3,4] which can mask or destroy the quantum effects. But in recent years, it has been shown how the coupling to an environment can be harnessed to generate useful quantum states [5–9] or perform quantum information tasks [9,10]. Moreover, the study of the phase diagram of open quantum systems has turned into a fruitful direction itself [11–16].

Our aim in the present work is twofold: In the first part of the paper, we propose a scheme to realize a quantum spin system using ultracold atoms in an optical lattice in which both coherent interaction and dissipation can be engineered and controlled, enabling the study the nonequilibrium and steady-state physics of open and driven spin systems. In the second part, we highlight a peculiar feature of the steady-state diagram for small spin chains: in the limit of weak dissipation, abrupt changes of steady-state expectation values for certain critical values of the system parameters are observed. We explain this feature and relate it to degeneracy properties of the system Hamiltonian and derive a sufficient condition for the occurrence of sharp peaks at critical system parameters.

II. PHYSICAL IMPLEMENTATION OF ONE-DIMENSIONAL SPIN CHAIN UNDER DISSIPATION

Ultracold bosonic atoms in optical lattices are ideal candidates to simulate spin Hamiltonians. Different theoretical and experimental approaches [17] have been employed to simulate quantum spin chains in optical lattices; for example, by optical driving of two hyperfine levels of cold bosons in the Hubbard regime [18]. Recently, a one-dimensional chain of interacting Ising spins has been implemented experimentally using a Mott-Insulator of spinless bosons in a tilted optical lattice [19].

In the following, we show theoretically how to add engineered dissipation to the toolbox of these systems [20,21]. Specifically, we show how to implement a system with the following properties: (i) dissipative dynamics of Lindblad form, (ii) a tunable magnetic field in x direction and (iii) an effective spin Hamiltonian such as, e.g., the XXZ, Heisenberg, or Ising model. In the next sections, we first introduce the setup and explain qualitatively how such a one-dimensional spin chain in a tunable magnetic field under engineerable dissipation can be realized with cold atoms in optical lattices. In the subsequent sections we give specific requirements and parameters and details of the derivation for (i)–(iii).

A. Setup and qualitative description

The system we consider is an optical lattice populated with a single atomic bosonic species. We assume to be in the Mott-insulator regime with filling factor 1, where the on-site interaction is much larger than the tunneling (hopping) between neighboring lattice sites. In this regime, the atoms are localized such that each lattice potential is occupied with one atom. We aim to use the motional ground and first-excited state of the atom (denoted by $|0\rangle$ and $|1\rangle$ [22], respectively) to realize an effective spin-$\frac{1}{2}$ system in each lattice site. To access the motional degree of freedom optically, we work in the Lamb-Dicke regime where the motion of the atom is restricted to a region small compared with the laser wavelength. We make use of the anharmonicity of the lattice potential and, as explained in the following, of decay of the atoms that leads to cooling of the system, to restrict the dynamics to the two-dimensional subspace of $\{|0\rangle,|1\rangle\}$ [23] (see Fig. 1). For the optical manipulation, we assume that the atoms have internal degrees of freedom that can be addressed with laser fields. We consider a Λ scheme with two ground states $|g\rangle$ and $|r\rangle$ (both trapped by the same optical lattice potential) and an excited state $|e\rangle$. The level scheme of the internal states of the atoms

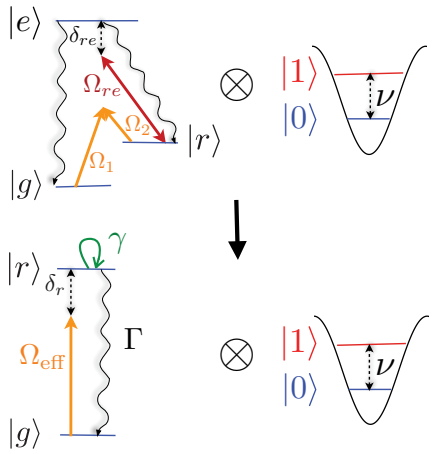

FIG. 1. (Color online) Relevant level structure and coupling and decay terms of single atom trapped at a lattice site. The upper-left part shows the internal levels of the atom: Λ system $|g\rangle$, $|r\rangle$, $|e\rangle$, off-resonantly driven by lasers. The right part shows motional states in the lattice potential. Lower part: After adiabatic elimination of $|e\rangle$, an effective two-level system with tunable decay rate Γ and dephasing rate γ is obtained.

is shown in Fig. 1. Off-resonant laser fields drive transitions between the two ground states $|g\rangle$ and $|r\rangle$ and the excited state $|e\rangle$. The system decays fast into the ground states and, as we show below, effectively decays into the state $|g\rangle$. Therefore, the atoms are optically pumped to the state $|g\rangle \otimes |0\rangle$ and the states $|r\rangle$ and $|e\rangle$ can be adiabatically eliminated. Eliminating the excited state $|e\rangle$ leads to the effective two-level system in the lower part of Fig. 1 with designable decay rates. Further elimination of the state $|r\rangle$ leads to an effective description in the internal ground state $|g\rangle$ (see Fig. 2). The optical couplings by laser fields give rise to effective Hamiltonians and effective dissipation (cooling) in the ground state $|g\rangle$ at each lattice site. Details are given in Sec. II B. In summary, we obtain an effective two-level system at each lattice site with Hilbert space spanned by $|g\rangle \otimes |0\rangle$ and $|g\rangle \otimes |1\rangle$ as depicted in Fig. 3.

In the following sections, we show that engineering the optical couplings as above leads to an effective master equation

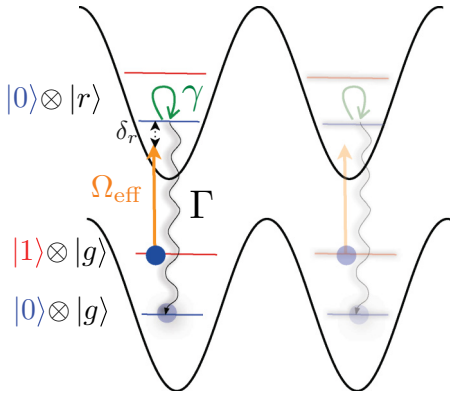

FIG. 2. (Color online) Effective two-level system $|g\rangle$-$|r\rangle$ in the optical lattice potential with motional states $|0\rangle$ and $|1\rangle$. Choosing resonance conditions as explained in Sec. II B, the atoms are selectively excited from $|g\rangle \otimes |1\rangle$ to the state $|r\rangle \otimes |0\rangle$ and spontaneously decay into $|g\rangle \otimes |0\rangle$.

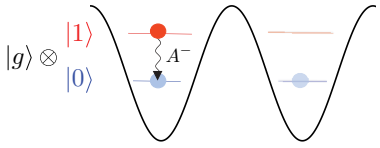

FIG. 3. (Color online) Decay of the effective two-level system $\{|0\rangle\},\{|1\rangle\}$ as described by the effective master equation derived in Sec. II B. The dissipation strength A^- is given in Eq. (7).

for the two-level system $|0\rangle$, $|1\rangle$ that describes (i) decay from $|1\rangle$ to $|0\rangle$ and (ii) an effective magnetic field in x direction. In the Mott insulator regime, tunnel couplings between neighboring lattice wells can be treated as a perturbation, which (iii) leads to an effective spin Hamiltonian. The resulting master equation [24] is given by

$$\dot{\rho}_t = \sum_k A^-(2\sigma_k^- \rho_t \sigma_k^+ - \{\sigma_k^+\sigma_k^-, \rho_t\}_+) - i[H, \rho_t]. \qquad (1)$$

Here, $\sigma_k^+ = |1\rangle\langle 0|_k$ is the operator that excites an atom at lattice site k from the motional state $|0\rangle$ to state $|1\rangle$ and $\sigma_k^- = (\sigma_k^+)^\dagger$. The sum runs over all N sites of the optical lattice potential. The first part in Eq. (1) describes decay from state $|1\rangle$ into state $|0\rangle$ as depicted in Fig. 3. It is derived in Sec. II B. The decay parameter A^- can be tuned by changing the Rabi frequencies of the lasers and the detunings and is given by Eq. (18) in Sec. II E. The Hamiltonian is given by $H = H_B + H_{\text{spin}}$, where H_B describes the magnetic field in x direction given by

$$H_B = \sum_k B_x(\sigma_k^+ + \sigma_k^-), \qquad (2)$$

where B_x is proportional to an effective magnetic field in the x direction. It is derived in Sec. II C. The Hamiltonian H_{spin} describes the spin Hamiltonian

$$H_{\text{spin}} = \sum_k \alpha_1\left(\sigma_k^x \sigma_{k+1}^x + \sigma_k^y \sigma_{k+1}^y\right) + \alpha_2 \sigma_k^z \sigma_{k+1}^z, \qquad (3)$$

as derived in Sec. II D. The parameters α_1 and α_2 depend on the properties of the optical lattice potential and can be tuned. Therefore, the Hamiltonian H_{spin} describes the XXZ model, the Ising model, or the Heisenberg model. In the following three sections, we employ a perturbative approach to derive a master equation comprising dissipation of Lindblad form (i) as in Eq. (1), a magnetic field in x direction (ii) as in Eq. (2), and an effective spin Hamiltonian (iii) as in Eq. (3). For the sake of clarity, we derive (i)–(iii) in three separate steps employing the approximation of independent rates of variation as explained in Ref. [25].

B. Optical couplings of internal atomic states: dissipation of Lindblad form

In this section, we show that optically addressing the atoms with suitably tuned lasers allows to engineer decay as in Eq. (1).

We consider the internal levels $|g\rangle$, $|r\rangle$, $|e\rangle$ of an atom at site k. The ground states $|g\rangle$ and $|r\rangle$ can be coupled via the excited state $|e\rangle$ by a detuned Raman transition of two standing-wave laser fields with Rabi frequencies Ω_1 and Ω_2. Eliminating the excited state $|e\rangle$ leads to an effective coupling between $|g\rangle$

and $|r\rangle$ (see Fig. 1) with $\Omega_{\text{eff}} = \Omega_1\Omega_2/\delta_{re}$ where δ_{re} is the detuning with respect to $|e\rangle$ (for details see Appendix A). To induce controlled dissipation, we couple $|r\rangle$ and $|e\rangle$ by an additional off-resonant laser field (indicated by a red arrow) in Fig. 1. Then adiabatic elimination of the excited state $|e\rangle$ leads to an effective two-level system (as shown in the lower part of Fig. 1) with states $|r\rangle$ and $|g\rangle$ which has designable decay rates Γ and γ as derived in [26] (see also Appendix A). Thereby, the excited state $|e\rangle$ that is broadened by spontaneous emission is eliminated, and the effective two-level system $|g\rangle$-$|r\rangle$ allows the motional states $|0\rangle$ and $|1\rangle$ of the lattice potential to be resolved (note that we are in the Lamb-Dicke regime), as can be seen in Fig. 2. Under appropriate resonance conditions that will be specified in the following, the atoms are excited from state $|1\rangle \otimes |g\rangle$ to state $|0\rangle \otimes |r\rangle$ and spontaneously decay into the state $|0\rangle \otimes |g\rangle$ as shown in Fig. 2. Adiabatically eliminating the state $|r\rangle$, this corresponds to an effective decay from state $|1\rangle \otimes |g\rangle$ into $|0\rangle \otimes |g\rangle$. Thus the atoms effectively remain in the internal ground state $|g\rangle$, such that the decay can be written as an effective decay from state $|1\rangle$ to $|0\rangle$ as depicted in Fig. 3.

In Appendix A, we derive in a perturbative approach (that corresponds to an adiabatic elimination of the state $|r\rangle$) a master equation that describes the dynamics of the two-level system $|0\rangle$, $|1\rangle$ of the atom. Assuming that the driving of level $|r\rangle$ is sufficiently weak such that

$$|\Omega_{\text{eff}}| \ll \Gamma, \gamma, \nu, |\delta_r|, \tag{4}$$

and that the level broadening remains small

$$\Gamma + \gamma < \nu, \tag{5}$$

the master equation is given by

$$\dot{\rho}_t = \sum_k A^-(2\sigma_k^-\rho_t\sigma_k^+ - \{\sigma_k^+\sigma_k^-, \rho_t\}_+) + A^+(2\sigma_k^+\rho_t\sigma_k^- - \{\sigma_k^-\sigma_k^+, \rho_t\}_+) - i\big[H_{\text{eff}}^{(1)}, \rho_t\big]. \tag{6}$$

Here, A^+ determines the strength of the heating terms and A^- the strength of the decay terms. For simplicity, $A^\pm$ are chosen to be independent of the lattice site k. $A^\pm$ can be made dependent on the lattice site k by choosing different phases of the driving lasers as explained in Appendix A. Note that $A^+ \ll A^-$ is required for the validity of the approximation that restricts to the $|0\rangle$ and $|1\rangle$ subspace. A^- and A^+ are given by

$$A^\pm = \Omega_{\text{eff}}^2\eta_1^2 \frac{(\Gamma + \gamma)}{(\Gamma + \gamma)^2 + (\delta_r \pm \nu)^2}. \tag{7}$$

Here, δ_r is the effective detuning given by Eq. (A5) in Appendix A, $\eta_1 = k_1/\sqrt{2M\nu}$ is the Lamb-Dicke parameter where k_1 is the wave number of the laser with Rabi frequency Ω_1, M is the atomic mass, and ν denotes the energy difference between the motional state $|0\rangle$ and $|1\rangle$ of the lattice potential. The Hamiltonian $H_{\text{eff}}^{(1)}$ in the last term in Eq. (6) is given by

$$H_{\text{eff}}^{(1)} = \sum_k \nu|1\rangle\langle 1|_k + H_S, \tag{8}$$

where H_S describes ac Stark shifts on the motional levels that are $\ll\nu$ and are given in more detail in Appendix A. Now we have everything at hand to implement dissipation. If

$$\delta_r \approx \nu,$$

which can be achieved by choosing the laser frequency ω_l in $\delta_r = \omega_r - \omega_l$ accordingly, the strength of the dissipation is much larger than the strength of the heating:

$$A^+ \ll A^-. \tag{9}$$

Then, the master equation has only decaying terms and is of the form

$$\dot{\rho}_t = \sum_k A^-(2\sigma_k^-\rho_t\sigma_k^+ - \{\sigma_k^+\sigma_k^-, \rho_t\}_+) - i\big[H_{\text{eff}}^{(1)}, \rho_t\big]. \tag{10}$$

It describes decay of the atoms from state $|1\rangle$ into $|0\rangle$, while the atoms effectively remain in the internal state $|g\rangle$. By adiabatic elimination of the internal state $|r\rangle$, we have thus shown that a master equation can be derived that can be tuned such that it describes almost pure decay.

C. Optical couplings of internal atomic states: Effective magnetic field in x direction

To derive the effective magnetic field in x direction, we consider a detuned Raman transition. Two standing-wave laser fields with Rabi frequencies Ω_a and Ω_b couple the internal ground state $|g\rangle$ and the excited state $|e\rangle$ of the atoms, as depicted in Fig. 4. The coupling is described by the Hamiltonian

$$H_{ab} = \sum_k \Omega_a \cos(k_a x_k)|e\rangle\langle g|_k + \Omega_b \sin(k_b x_k)|e\rangle\langle g|_k + \text{H.c.}, \tag{11}$$

where k_a, k_b denote the wave numbers of the lasers and x_k is the displacement from the equilibrium position of the atom at lattice site k. As we are in the Lamb-Dicke regime, $\sin(k_b x_k) \approx \eta_b(\sigma_k^- + \sigma_k^+)$ [27] and $\cos(k_a x_k) \approx 1$. Under the condition

$$|\Omega_a|, |\Omega_b| \ll |\delta_e|, \tag{12}$$

where δ_e is the detuning of the driving lasers, as depicted in Fig. 4, the excited state $|e\rangle$ can be adiabatically eliminated and we get an effective Hamiltonian

$$H_{\text{eff}}^{(2)} = H_B = \sum_k B_x\sigma_k^x, \tag{13}$$

which describes a tunable magnetic field in x direction, where B_x is proportional to the effective magnetic field strength in x direction, which is given by

$$B_x = \frac{2\Omega_a\Omega_b\eta_b}{\delta_e}.$$

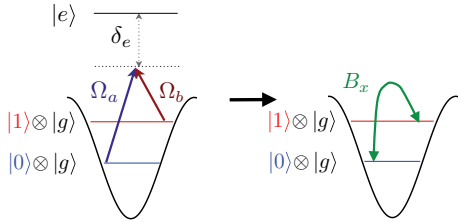

FIG. 4. (Color online) Level scheme and transitions used to implement the transverse magnetic field. Left: A detuned Raman transition couples the internal ground state $|g\rangle$ and the excited state $|e\rangle$ of the atom. Right: Adiabatic elimination of the excited state $|e\rangle$ leads to an effective magnetic field in x direction (see Sec. II C), which drives transitions between the motional states $|0\rangle$ and $|1\rangle$.

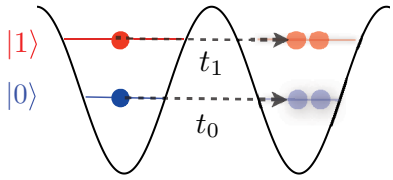

FIG. 5. (Color online) Tunneling between neighboring lattice wells with tunnel amplitudes t_0 and t_1. States with two atoms per lattice well are treated in perturbation theory in Sec. II D, as the on-site interaction is much larger than the tunneling amplitudes.

Thus, we have derived an effective magnetic field in x direction that drives transitions between the motional states $|0\rangle$ and $|1\rangle$ (as depicted on the right side of Fig. 4), while the atoms remain in the internal ground state $|g\rangle$.

D. Effective spin Hamiltonian

In the Mott-insulator regime, bosonic atoms trapped by a lattice potential with two motional states are described by the two-band Bose-Hubbard model [28] (see Appendix B). We denote the on-site interaction by U_{01}, U_{00}, and U_{11} [29] and by t_0 (t_1) the amplitudes for atoms in state $|0\rangle$ ($|1\rangle$) to tunnel to neighboring lattice sites. We assume that the on-site interaction $U_{01}, U_{00}, U_{11} \gg t_0, t_1$ such that tunneling between neighboring wells, which leads to states with two atoms in one lattice well, can be treated as a perturbation (see Fig. 5). Using second-order perturbation theory [25] (for a detailed derivation see Appendix B), we derive an effective spin Hamiltonian $H_{\rm spin}$ given by

$$H_{\rm eff}^{(3)} = H_{\rm spin} + B_z \sum_k |1\rangle\langle 1|_k, \tag{14}$$

with

$$H_{\rm spin} = \sum_k \alpha_1 \left(\sigma_k^x \sigma_{k+1}^x + \sigma_k^y \sigma_{k+1}^y\right) + \alpha_2 \sigma_k^z \sigma_{k+1}^z, \tag{15}$$

where $\alpha_1 = -4t_0 t_1/U_{01}, \alpha_2 = 2[(t_0^2+t_1^2)/(2U_{01}) - t_0^2/U_{00} - t_1^2/U_{11}]$, and the magnetic field in z direction is

$$B_z = t_0^2/U_{00} - t_1^2/U_{11}, \tag{16}$$

using the Pauli spin matrices σ_k^x, σ_k^y with $\sigma_k^x = (|0\rangle\langle 1|_k + |1\rangle\langle 0|_k)/2$. The Hamiltonian given by Eq. (14) is an effective spin Hamiltonian that is tunable by changing the lattice properties. If $\alpha_1, \alpha_2 > 0$, $H_{\rm eff}^{(3)}$ corresponds to the XXZ model with a magnetic field in z direction. If the lattice properties can be tuned such that one of the tunneling constants t_0 or $t_1 \to 0$, $H_{\rm spin}$ is an Ising Hamiltonian with a magnetic field in z direction. For $\alpha_1 = \alpha_2$, $H_{\rm spin}$ corresponds to the Heisenberg model.

E. Dissipative one-dimensional spin chain in magnetic field

In the previous sections, we showed—for the sake of clarity in separate steps—that optical couplings of the internal levels can be engineered such that we obtain a master equation of Lindblad form [Eq. (6)] fulfilling the demands (i)–(iii) of tunable dissipation, spin-interaction, and tunable transverse field. Combining these results, one has to carefully consider the order of magnitude of each term. Doing so, we find that the magnetic field B_z in z direction in Eq. (14) and the Stark shifts in Eq. (8) can be of the same order of magnitude as ν. Stark shifts and B_z lead to an effective energy difference between the motional states $|0\rangle$ and $|1\rangle$ given by

$$\tilde{\nu} = \nu + B_z + s_- - s_+,$$

where B_z is defined in Eq. (15) and s_-, s_+ are the ac Stark shifts in Eq. (8) (see Appendix A). Therefore, combining all results, the laser detuning δ_r that enters in $A^\pm$ has to be adjusted to $\tilde{\delta}_r$ such that $\tilde{\delta}_r - \nu = \delta_r - \tilde{\nu}$, which means that $\tilde{\delta}_r = \delta_r \pm (B_z + s_- - s_+)$.

Then, combining the results from Eqs. (6), (13), and (14), the master equation reads

$$\dot{\rho}_t = \sum_k A^+(2\sigma_k^+\rho_t\sigma_k^- - \{\sigma_k^-\sigma_k^+, \rho_t\}_+) + A^-(2\sigma_k^-\rho_t\sigma_k^+ - \{\sigma_k^+\sigma_k^-, \rho_t\}_+) - i[H, \rho_t], \tag{17}$$

where the rates $A^\pm$ are modified by the renormalized $\tilde{\delta}_r$:

$$A^\pm = \Omega_{\rm eff}^2 \eta_1^2 \frac{(\Gamma+\gamma)}{(\Gamma+\gamma)^2 + (\tilde{\delta}_r \pm \nu)^2}. \tag{18}$$

The Hamiltonian part of the master equation is given by

$$H = H_{\rm spin} + H_B + \tilde{\nu} \sum_k |1\rangle\langle 1|_k, \tag{19}$$

where $H_{\rm spin}$ is given by Eq. (15) and H_B by Eq. (13). The magnetic field in z direction and Stark shifts have been included in $\tilde{\nu}$. For $\tilde{\delta}_r \approx \nu$, as shown before, decay dominates over heating: $A^- \gg A^+$. Then, the master equation has only decaying terms and Eq. (17) describes a dissipative XXZ spin chain in a magnetic field with both x and z components. However, only B_x is fully tunable, while B_z is large (compared to B_x, $A^\pm$) and required to be so by the conditions for adiabatic elimination, cf. Eq. (4). However, an effective dissipative XXZ chain without any field in z direction would be advantageous for observing critical behavior in the steady-state dynamics that we study in the next sections. Therefore, we transform to a frame rotating with $\tilde{\nu}$. In the rotating frame, H_B becomes time dependent. To obtain a time-independent field in x direction, the detuned Raman lasers that lead to the effective magnetic field B_x have to be chosen time dependent, adapted to the rotating frame (i.e., suitably detuned from the two-photon resonance). This then yields a time-independent transversal magnetic field, and the master equation in the rotating frame is then given by

$$\dot{\rho}_t = \sum_k A^-(2\sigma_k^-\rho_t\sigma_k^+ - \{\sigma_k^+\sigma_k^-, \rho_t\}_+) - i[H_{\rm spin} + H_B, \rho_t]. \tag{20}$$

It corresponds to the master equation given by Eq. (1). In summary we have shown how to implement a one-dimensional spin chain with nearest-neighbor interaction described by the XXZ or the Ising model and a tunable effective magnetic field in x direction under dissipation. This system is an ideal test bed for studying steady-state dynamics of dissipative spin models, as discussed in the next section. Note that since we are in a rotating frame, observables other than the collective spin operator $\langle J_z\rangle$ become explicitly time dependent.

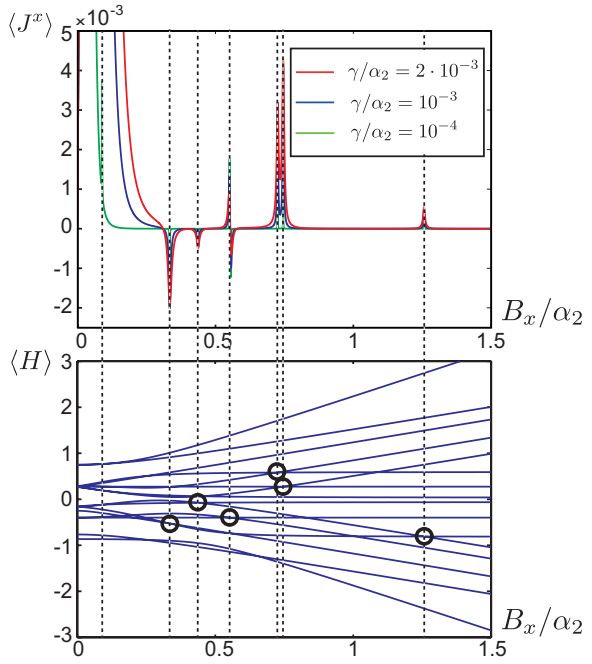

FIG. 6. (Color online) XXZ model with 4 spins, $\alpha_1 = \frac{1}{4}\alpha_2$ and open boundary conditions under local dissipation of form given by Eq. (20). Upper part: Steady-state expectation value $\langle J^x \rangle$ plotted versus the magnetic field B_x/α_2. Peaks are observed that narrow for decreasing the dissipation strength. Lower part: Spectrum of XXZ chain in the magnetic field B_x plotted versus B_x/α_2. Peaks in the steady-state expectation value (upper part) appear at crossing points of the Hamiltonian that are marked with black circles.

F. Steady-state behavior: Discontinuous steady-state behavior related to spectrum of Hamiltonian

A particular important characterization of dissipative dynamics is through their steady state: if it is unique (or distinguished by some conserved quantity) it allows for robust preparation of these states. Abrupt changes in the steady state as system parameters are varied may signal dissipative quantum phase transitions [12–16,30,31]. We study the steady-state behavior of short spin chains under dissipation in a magnetic field in the x direction by numerical simulations. We find that the one-dimensional XXZ model with four spins, as given by Eq. (15) where we chose as a typical example $\alpha_1 = \frac{1}{4}\alpha_2$, shows a surprising behavior: Changing the external magnetic field in the x direction makes peaks occur in the steady-state expectation values of the collective spin operators $J^{x/z} = \sum_k \sigma_k^{x/z}$ for weak dissipation; see Fig. 6. Here, we considered dissipation as in Eq. (20) with equal dissipation strength on each spin. We find that, upon decreasing the strength of the dissipation, the peaks become more narrow and each peak height approaches a finite value. For small γ we observe very narrow peaks. This indicates a discontinuity in the steady-state expectation values of the spin operators. We find that these narrow peaks appear exactly at points where the Hamiltonian becomes degenerate. In the following section we study this phenomenon in more generality.

III. DISCONTINUITIES IN STEADY-STATE DYNAMICS OF GENERAL CLASS OF ONE-DIMENSIONAL SPIN MODELS UNDER DISSIPATION

In the previous section we saw that, for the one-dimensional XXZ model, peaks in the steady-state expectation values of the collective spin operators appear, that are closely related to the spectrum of the Hamiltonian. In the following, we study in more generality and independent of a physical implementation local one-dimensional spin Hamiltonians under dissipation of different kinds. We present a condition that elucidates the discontinuous behavior of the steady state at degeneracy points of the Hamiltonian. Next, we study and explain this condition in more detail for Ising Hamiltonians.

A. Numerical studies of discontinuous behavior in steady state

We numerically simulate short spin chains. First, we study the one-dimensional Ising model with open boundary conditions, described by the Hamiltonian

$$H = H_{zz} + H_B, \tag{21}$$

with

$$H_{zz} = \alpha_3 \sum_k \sigma_k^z \sigma_{k+1}^z, \tag{22}$$

and H_B as in Eq. (2) subject to local or collective decay with Lindblad operators $\propto \sigma_k^-$ or $\sum_k \sigma_k^-$, respectively. The master equation describing the full system with local dissipation is given by

$$\dot{\rho}_t = \sum_k \gamma_k (2\sigma_k^- \rho_t \sigma_k^+ - \{\sigma_k^+ \sigma_k^-, \rho_t\}_+) - i[H, \rho_t]. \tag{23}$$

Changing the magnetic field B_x, we find that for weak dissipation the steady-state expectation values of the spin operators $\langle J^x \rangle$ and $\langle J^z \rangle$ change abruptly at particular values of B_x; see Fig. 7. Here, we considered dissipation as in Eq. (23) with equal dissipation strength on each spin, $\gamma_k = \gamma$. Upon decreasing the strength of the dissipation, i.e., decreasing γ, the peaks become more narrow and their height converges to some finite value, while the expectation value vanishes elsewhere. For $\gamma \to 0$, we observe very narrow peaks, which indicates discontinuities in the steady-state expectation values of the spin operators. We find that these narrow peaks appear only at degeneracy points of the spectrum of the Hamiltonian. That is, for every peak found at some value of $B_x = x_0$ for $\gamma \to 0$, at least one pair of degenerate eigenvalues λ_1, λ_2 of the local spin Hamiltonian H_{zz} can be found, i.e., $\lambda_1(x) = \lambda_2(x)$ at $x = x_0$. Note that the discontinuities in the steady state at critical system parameters are only observed for $\gamma \neq 0$. That is, the (weak) dissipation allows us to gain information about the Hamiltonian's properties that is not readily accessible in the case of $\gamma = 0$.

This effect can be observed for different kinds of spin Hamiltonians such as, for example, the XXZ model (see Fig. 6), both for periodic and open boundary conditions. Moreover, changing the type of dissipation, the observed behavior does not change qualitatively. For example, collective dissipation, which describes the dynamics of spins all coupled to the same bath and leads to the master equation

$$\dot{\rho}_t = \gamma (2J^- \rho_t J^+ - \{J^+ J^-, \rho_t\}_+) - i[H, \rho_t], \tag{24}$$

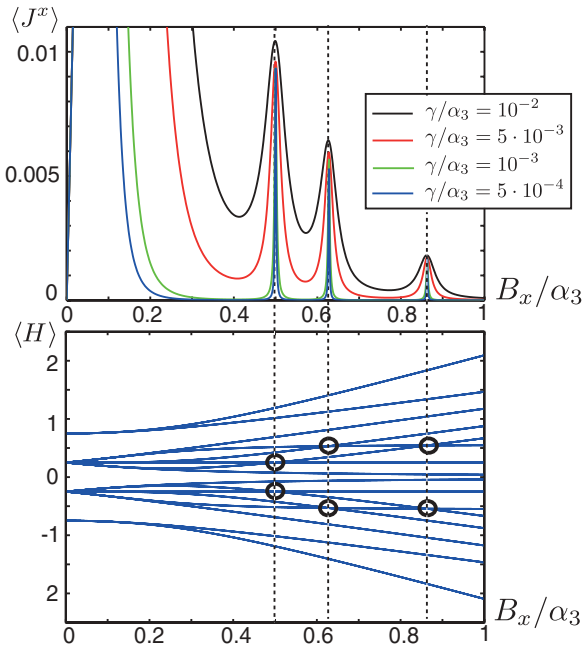

FIG. 7. (Color online) Ising model with 4 spins with open boundary conditions in a transverse magnetic field B_x and under local dissipation of form given by Eq. (23). Upper part: Steady-state expectation value $\langle J^x \rangle$ plotted versus B_x/α_3. Peaks are observed that become more narrow for decreasing dissipation strength. Lower part: Spectrum of the Hamiltonian plotted versus B_x/α_3. Peaks in the steady-state expectation value (upper part) appear at degeneracy points of the Hamiltonian that are marked with black circles.

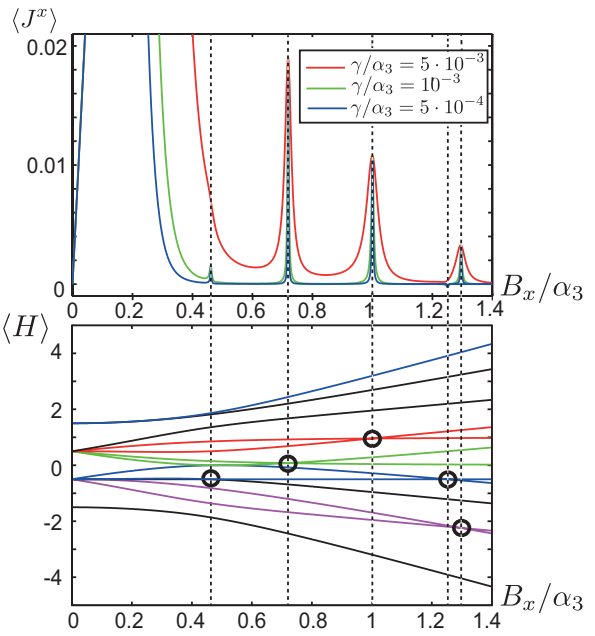

FIG. 8. (Color online) Ising model with 6 spins with periodic boundary conditions in a magnetic field B_x and under collective dissipation of the form given by Eq. (24) in the translation and reflection symmetric subspace $T = R = 1$. Upper part: Steady-state expectation value $\langle J^x \rangle$ plotted versus B_x/α_3. Lower part: Spectrum of the Hamiltonian plotted versus B_x/α_3.

where $J^{\pm} = \sum_k \sigma_k^{\pm}$ also leads to discontinuous behavior in the steady-state expectation values, as shown in Fig. 8 for the Ising model. Choosing an "inhomogeneous" dissipation which is of the form of the dissipative part in Eq. (23), where now the strengths of the dissipation γ_k are different for each spin, peaks can be observed for an even larger class of spin Hamiltonians: For $\gamma_k = \gamma$ and $H = H_H + H_B$, where H_H is the Heisenberg spin Hamiltonian, we do not observe any peaks. However, if we choose different dissipation strengths γ_k for each spin, we find peaks at the degeneracy points of the Hamiltonian, as can be seen in Fig. 9.

B. General condition for discontinuities in steady state

Since the Liouvillian depends smoothly on the system parameters, the observed discontinuities must be related to degeneracies in the spectrum of $\mathcal{L}$. As we shall see, in the weak-dissipation limit they are directly related to degeneracy points of the Hamiltonian.

We consider a system described by the master equation

$$\dot{\rho}(t) = \mathcal{L}\rho \equiv [\mathcal{L}_0(x) + \gamma \mathcal{L}_1]\rho(t), \tag{25}$$

where

$$\mathcal{L}_0(x)(\rho) = -i[H(x), \rho],$$

with a Hamiltonian $H(x)$ depending (analytically) on a parameter x. For simplicity, we consider the case in which $H_0(x)$ is nondegenerate for $x \neq x_0$. The term $\mathcal{L}_1$ contains dissipative terms and is independent of x. We are interested in the limit of weak dissipation ($\gamma \to 0$) and in the change of the steady state at the degeneracy point $x = x_0$.

The steady state $\rho_{\rm ss}(x)$ is determined by $\mathcal{L}(x)\rho_{\rm ss}(x) = 0$ and can be determined perturbatively. The kernel of $\mathcal{L}_0(x)$ is highly

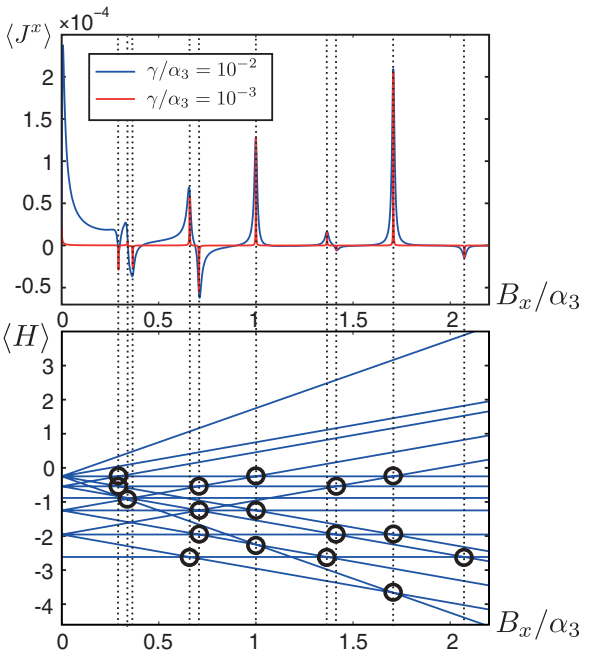

FIG. 9. (Color online) Heisenberg model with 4 spins with open boundary conditions in a magnetic field B_x and under local dissipation as given by Eq. (23) with different dissipation strengths γ_k. Upper panel: steady-state expectation value $\langle J^x \rangle$ plotted versus the B_x/α_3. Lower part: Spectrum of the Hamiltonian plotted versus B_x/α_3.

degenerate, being spanned by all eigenprojectors $|\lambda_i(x)\rangle\langle\lambda_i(x)|$ of the (nondegenerate) $H_0(x)$. This degeneracy is lifted by $\mathcal{L}_1$ and the steady state for $\gamma \to 0$ is for $x \neq x_0$ given by

$$\mathrm{P}^D(x)\mathcal{L}_1\mathrm{P}^D(x)\rho_{ss}(x) = 0, \tag{26}$$

where

$$\mathrm{P}^D(x)\rho = \sum_i |\lambda_i(x)\rangle\langle\lambda_i(x)|\rho|\lambda_i(x)\rangle\langle\lambda_i(x)|. \tag{27}$$

The possibility of discontinuous behavior of $\rho_{\rm ss}(x)$ at $x = x_0$ arises from the enlargement of the kernel of $\mathcal{L}_0(x)$ at this point: if λ_i and λ_j become degenerate at $x = x_0$ then coherences between the corresponding eigenvectors [i.e., $|\lambda_i(x)\rangle\langle\lambda_j(x)|, i \neq j$] become stationary at $x = x_0$. We denote by P^Δ the projector on these additional elements in the kernel of $\mathcal{L}_0(x_0)$ [32]. As we show in Appendix C, a discontinuity $\rho_{\rm ss}(x_0) \neq \lim_{x\to x_0}\rho_{\rm ss}(x)$ arises if

$$\mathrm{P}^\Delta\mathcal{L}_1 \lim_{x\to x_0}\rho_{ss}(x) \neq 0, \tag{28}$$

i.e., if $\mathcal{L}_1$ couples the steady state to the newly available subspace P^Δ in the kernel of $\mathcal{L}_0$. For simplicity, we made the assumption that the Hamiltonian is nondegenerate for $x \neq x_0$. If the Hamiltonian does have degeneracies outside x_0, but additional eigenvectors become degenerate at $x = x_0$ the argumentation follows identical lines, as also in this case, $\mathcal{L}_1$ can couple the steady state to a newly available subspace P^Δ.

Let us have another look at Figs. 6–9 in the light of the previous paragraph. Clearly, all the sharp isolated peaks occur for values of B_x (which plays the role of the parameter x), at which a degeneracy occurs, satisfying a necessary condition for Eq. (28). However, not all degeneracy points lead to discernible peaks, e.g., in Fig. 6. This can show that $\mathcal{L}_1$ does not couple the steady state to P^Δ or that the discontinuity is not witnessed by the expectation value of J^x. For most peaks studied here, however, the reason is simply that the corresponding peaks are too small and sharp to be resolved in the plot.

These points are illustrated in Fig. 10, which shows that the steady state changes abruptly at all degeneracy points of H for the four-spin XXZ model with local dissipation except for two such points (at $B_x \approx 0.16, 0.24$), where $\mathcal{L}_1$ does not couple to the coherences. To measure how quickly $\rho_{\rm ss}$ changes with B_x we use (in analogy to the ground-state fidelity introduced in Ref. [33] for the study of quantum phase transitions) the "steady-state infidelity" $I_{\delta B}(B_x) \equiv 1 - F(\rho(B_x), \rho(B_x + \delta B))$. Here $F(\rho,\sigma) = \mathrm{tr}[(\sigma^{1/2}\rho\sigma^{1/2})^{1/2}]^2 \in [0,1]$ denotes the Uhlmann fidelity [34] between two density matrices, which measures how similar ρ and σ are. Peaks in $I_{\delta B}(B_x)$ (for small δB) indicate that the steady state changes abruptly with B_x. For weak dissipation this happens close to all degeneracy points of the Hamiltonian when Eq. (28) holds.

Note also that, in Figs. 6–9, a large feature appears in the steady-state expectation value $\langle J^x\rangle$ around $B_x = 0$. It narrows for decreasing γ, but is not a sharp peak for any of the parameters used for γ. This broad peak represents the effect of one (or several, cf. Figs. 6 and 9) unresolved degeneracies around $B_x = 0$: Note that for all spin models considered, the degeneracy of their respective Hamiltonian is very high at $B_x = 0$ and is lifted slowly (certain eigenvalues touch and do not cross as $B_x \to 0$). Therefore, the finite values of γ used in the plots are not much smaller than all energy differences and we are not in the weak-dissipation limit. As γ is reduced, additional peaks are resolved (cf. Fig. 9).

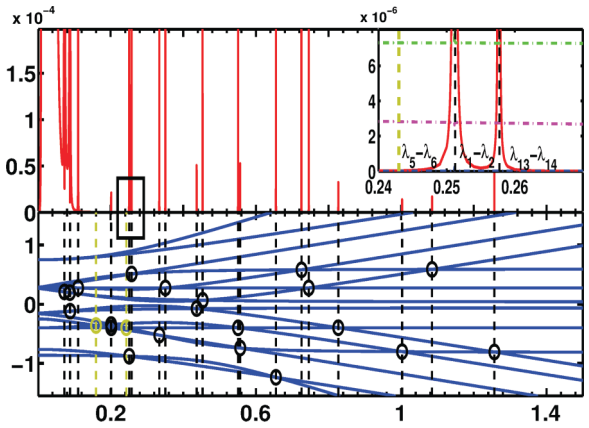

FIG. 10. (Color online) (Upper part) Steady-state infidelity $I_{\delta B}(B_x)$ (see text) for the four-spin XXZ model in transverse field B_x with local dissipation (cf. Fig. 6) for $\delta B = 3 \times 10^{-6}$ and weak dissipation $\gamma = 0.5 \times 10^{-4}$. (Lower part) Spectrum of $H_{\rm spin}$, dashed vertical lines indicate degeneracy points (encircled). Peaks in $I_{\delta B}$ line up with degeneracy points of $H(B_x)$, except for two (colored green) for which condition (28) does not hold. The inset shows the vicinity of $B_x \approx 0.25$, where three crossings of eigenvalues occur: (λ_5,λ_6), (λ_1,λ_2), and $(\lambda_{13},\lambda_{14})$. The dash-dotted horizontal lines show the 2-norm (scaled by 7×10^{-7}) of the left-hand side of Eq. (28) $C_{i,j} = \|\mathrm{P}^{\Delta_{i,j}}\mathcal{L}_1 \lim_{x'\to x}\rho_{ss}(x')\|_2$ for the three relevant projectors $\mathrm{P}^{\Delta_{i,j}}$, $(i,j) = (1,2)$ (green), $=(5,6)$ (blue), and $=(13,14)$ (magenta). $C_{5,6}$ vanishes at the crossing of (λ_5,λ_6), hence there is no peak in $I_{\delta B}$, while the other two lead to a peak in $I_{\delta B}$, since $C_{i,j}$ is finite.

C. Steady-state behavior for Ising Hamiltonians

To get a better insight into how the condition given by Eq. (28) explains the peaks seen in Fig. 8, we now specialize to the Ising model under collective dissipation given by Eq. (24). Then we see that the steady state apart from the degeneracy points and the condition for discontinuity becomes very simple. For a detailed derivation of what follows, see Appendix C.

The Hamiltonian in Eq. (21) with periodic boundary conditions is in general degenerate due to translational and reflection symmetry. To obtain a nondegenerate H, we restrict our consideration to a specific subspace with eigenvalue 1 for the translation operator T and the reflection operator R [35]. Note that the Hamiltonian is also symmetric under the spin-flip operation $F = \sigma_x^{\otimes N}$, i.e., $FHF^\dagger = H$. Using the properties of $\mathcal{L}_1$ and F invariance of H, we find that, if the system has a unique steady state of $\mathcal{L}(x)$, it is, in the limit of weak dissipation, given by the maximally mixed state $\propto\mathbb{1}$: plugging $\mathbb{1}$ into Eq. (26) we obtain $\mathrm{P}^D\mathcal{L}_1(\mathbb{1}) = \sum_i |\lambda_i(x)\rangle\langle\lambda_i(x)|J^z|\lambda_i(x)\rangle\langle\lambda_i(x)|$ and flip invariance of H implies $\langle\lambda_i(x)|J^z|\lambda_i(x)\rangle = 0$ for the eigenstates of a nondegenerate Hamiltonian H (see Appendix C).

Thus if the steady state is unique, it is always maximally mixed outside degeneracy points and we see a discontinuity at $x = x_0$ if for the degenerate eigenstates $|\lambda_1(x_0)\rangle, |\lambda_2(x_0)\rangle$ we have

$$\langle\lambda_1|J^z|\lambda_2\rangle \neq 0. \tag{29}$$

This can be checked to hold for the points at which peaks are observed in Fig. 8.

For the Ising model in a transverse magnetic field, for larger N the peaks decrease in height and disappear in the limit $N \longrightarrow \infty$. The spectrum for the Ising model in a transverse field is known analytically [36]. For large N, the spectrum is very dense and degeneracy points are so closely spaced that peaks are no longer resolvable (and vanish in the thermodynamic limit as bands develop). Nevertheless, for small spin systems, these features provide a method to dissipatively study degeneracies of the applicable Hamiltonian—anywhere in the spectrum, not just in the ground state. To the extent that $\mathcal{L}_1$ is tunable, it even provides access to the nature of the degenerate states via Eq. (28).

IV. CONCLUSIONS

We have shown that using cold atoms in an optical lattice in the Mott-insulator regime, dissipative spin chains with Hamiltonians such as the XXZ model, the Ising model, or the Heisenberg model can be realized. Optical driving of internal atomic states allows for the realization of a tunable transversal magnetic field and engineered dissipation.

This system is an ideal test bed for studying steady-state dynamics of dissipative spin models. We have discovered a peculiar feature of the steady-state diagram for small spin chains: in the limit of weak dissipation, the expectation values of the collective spin operators exhibit abrupt changes that hint at discontinuities in the steady state. These discontinuities occur at degeneracy points of the Hamiltonian. We have studied this phenomenon for different spin models with open and periodic boundary conditions subject to individual and collective dissipation. Finally, we have presented conditions that elucidate the discontinuous behavior of the steady state at degeneracy points of the Hamiltonian. Therefore, measurements of the steady-state dynamics of cold atoms in optical lattices would allow us to draw conclusions about the spectrum of the respective spin model.

ACKNOWLEDGMENTS

H. S. and G. G. thank L. Mazza for useful discussions on cold atoms. The authors gratefully acknowledge funding by the DFG within the SFB 631 and by the EU within project MALICIA under FET-Open grant number 265522.

APPENDIX A: DERIVATION OF EFFECTIVE DISSIPATIVE MASTER EQUATION

The internal levels of the atom that we consider are $|g\rangle$, $|r\rangle$, $|e\rangle$. Adiabatically eliminating the excited state $|e\rangle$ as discussed in Sec. II B, we get an effective two-level system $|g\rangle$ and $|r\rangle$ that is coupled with the effective Rabi frequency Ω_{eff}, as depicted in Fig. 1.

In the following, we derive in detail the master equation given by Eq. (6) in Sec. II B. The internal levels of the atom that we consider are $|g\rangle$, $|r\rangle$, $|e\rangle$, as depicted in the upper part of Fig. 1. The states $|g\rangle$-$|r\rangle$ are coupled by a detuned Raman transition via the excited state $|e\rangle$ by two standing-wave laser fields. The coupling is described by the Hamiltonians

$$H_{l1} = \sum_k \Omega_1 \cos(k_1 x_k)(|e\rangle\langle g|_k + \text{H.c.}), \tag{A1}$$

and

$$H_{l2} = \sum_k \Omega_2 \sin(k_2 x_k)(|r\rangle\langle g|_k + \text{H.c.}), \tag{A2}$$

where Ω_1 and Ω_2 are the Rabi frequencies of the two lasers and k_1 and k_2 are the wave numbers of the lasers and k denotes the lattice site. x_k is the displacement from the equilibrium position x_k^0 of the atom at lattice site k. The phase of the lasers is, for simplicity, chosen such that $\cos[k_1(x_k + x_k^0)] = \cos(k_1 x_k)$ and $\cos[k_2(x_k + x_k^0)] = \sin(k_2 x_k)$. Choosing different phases of the lasers makes $A^{\pm}$ in Eq. (7) dependent on the lattice site k. Adiabatic elimination of the excited state $|e\rangle$ leads to an effective coupling

$$H_1 = \sum_k \Omega_{\text{eff}} \eta_1 (\sigma_k^- + \sigma_k^+)(|r\rangle\langle g| + \text{H.c.}), \tag{A3}$$

with $\Omega_{\text{eff}} = \Omega_1\Omega_2/\delta_{re}$ where δ_{re} is the detuning with respect to $|e\rangle$ and η_1 is the Lamb-Dicke parameter. Here, we have expressed the deviation from the equilibrium position x_k in terms of harmonic oscillator operators truncated to the two lowest-lying levels $\sin(k_1 x_k) \approx \eta_1(\sigma_k^- + \sigma_k^+)$ where $\sigma_k^+ = |1\rangle\langle 0|_k$ and $\sigma_k^- = |0\rangle\langle 1|_k$ and $\cos(k_2 x_k) \approx 1$. The effective coupling with Rabi frequency Ω_{eff} between states $|r\rangle$ and $|g\rangle$ is shown in Fig. 1.

Coupling the state $|r\rangle$ to the excited state $|e\rangle$ with a third standing-wave laser field with Rabi frequency Ω_{er}, depicted with a red arrow in Fig. 1, we can derive an effective two-level system $|g\rangle$-$|r\rangle$ with designable decay rates as done in Ref. [26]. Here, we briefly review this result. Following Ref. [26], the upper level $|e\rangle$ can be adiabatically eliminated if the saturation parameter for the transition $|r\rangle$ and $|e\rangle$ is small:

$$s_{r,e} = \frac{(\Omega_{re}/2)^2}{\delta_{re}^2 + (\Gamma_{er} + \Gamma_{eg})^2/4} \ll 1. \tag{A4}$$

According to Ref. [26], the effective detuning and the effective decay rates are given by

$$\delta_r = \delta_{gr} - \delta_{re}\frac{(\Omega_{re}/2)^2}{[(\Gamma_{eg} + \Gamma_{er})/2]^2 + \delta_{re}^2}, \tag{A5}$$

$$\Gamma = \frac{(\Omega_{re}/2)^2}{[(\Gamma_{eg} + \Gamma_{er})/2]^2 + \delta_{re}^2}\Gamma_{eg}, \tag{A6}$$

$$\gamma = \frac{(\Omega_{re}/2)^2}{[(\Gamma_{eg} + \Gamma_{er})/2]^2 + \delta_{re}^2}\frac{\Gamma_{eg} + \Gamma_{er}}{2}; \tag{A7}$$

see also the lower part of Fig. 1. The effective two-level system $|g\rangle$-$|r\rangle$ with the effective decay rates Γ, γ and the effective detuning δ_r is the starting point of the following discussion. The full Hamiltonian describing the system is given by

$$H_{\text{full}} = H_1 + H_0, \tag{A8}$$

where H_1 describes the atom-light interaction given by Eq. (A3) and H_0 defines the energies of the system

$$H_0 = \sum_k \delta_r |r\rangle\langle r|_k + \nu|1\rangle\langle 1|_k. \tag{A9}$$

The effective dynamics of the system can be derived considering contributions to the Liouvillian up to second order in a perturbative approach. The full system is described by a Liouvillian given by

$$\dot{\rho}(t) = (\mathcal{L}_0 + \mathcal{L}_1)\rho(t), \tag{A10}$$

where $\mathcal{L}_0$ is given by

$$\begin{aligned}\mathcal{L}_0\rho(t) = \sum_k \Gamma\,(2|g\rangle\langle r|_k\rho(t)|r\rangle\langle g|_k - \{|r\rangle\langle r|_k, \rho(t)\}_+) \\ + \gamma(2|r\rangle\langle r|_k\rho(t)|r\rangle\langle r|_k - \{|r\rangle\langle r|_k, \rho(t)\}_+) \\ - i[H_0, \rho(t)].\end{aligned} \tag{A11}$$

The first part of the Liouvillian is the decay part with the effective decay rate Γ from state $|r\rangle$ to $|g\rangle$ and the dephasing rate γ. The projector

$$P_g = |g\rangle\langle g| \otimes (|0\rangle\langle 0| + |1\rangle\langle 1|) \tag{A12}$$

is stationary under $\mathcal{L}_0$. The perturbative part of the Liouvillian is given by

$$\mathcal{L}_1\rho(t) = -i[H_1, \rho(t)], \tag{A13}$$

where H_1 is given by Eq. (A3) and describes the interaction of the two-level system with the effective laser field. Treating $\mathcal{L}_1$ as a perturbation, we derive an effective Liouvillian in the stationary subspace of $\mathcal{L}_0$. The projection onto this subspace reads

$$\mathbb{P}\dot{\rho}(t) = \mathbb{P}\mathcal{L}\mathbb{P}\rho(t) + \mathbb{P}\mathcal{L}\mathbb{Q}\rho(t), \tag{A14}$$

where $\mathbb{P}\rho = |g\rangle\langle g| \otimes (|0\rangle\langle 0| + |1\rangle\langle 1|)\rho|g\rangle\langle g| \otimes (|0\rangle\langle 0| + |1\rangle\langle 1|)$ and $\mathbb{Q} = 1 - \mathbb{P}$. Projecting onto the subspace we want to eliminate, we get

$$\mathbb{Q}\dot{\rho}(t) = \mathbb{Q}\mathcal{L}\rho(t). \tag{A15}$$

In the following, we integrate Eq. (A15) to get the time evolution of the density matrix in the fast space, $\mathbb{Q}\rho(t)$. We insert the result in Eq. (A14) to get an equation of motion for the density matrix in the slow space. Therefore, we first go into the interaction picture, where the density matrix is given by $\tilde{\rho}(t) = e^{-\mathcal{L}_0 t}\rho(t)$. The equation of motion in the fast space reads

$$\mathbb{Q}\dot{\tilde{\rho}}(t) = \mathbb{Q}W_I(t)\tilde{\rho}(t), \tag{A16}$$

with $W_I(t) = e^{\mathcal{L}_0 t}\mathcal{L}_1 e^{\mathcal{L}_0 t}$. Solving this equation by iteration [37], we get

$$\begin{aligned}\mathbb{Q}\rho(t) = \mathbb{Q}e^{\mathcal{L}_0 t}\left[\int_0^t ds\, W_I(s)\mathbb{P}\tilde{\rho}(0)\right. \\ \left. + \int_0^t ds_1 \int_0^{s_1} ds_2 W_I(s_1)W_I(s_2)\mathbb{P}\tilde{\rho}(0)\right].\end{aligned} \tag{A17}$$

At time $t = 0$, $\tilde{\rho}(0) = \rho(0)$ and we assume that at $t = 0$, the population is in the ground state, i.e., $\tilde{\rho}(0) = \mathbb{P}\tilde{\rho}(0)$. Higher-order integrals are neglected with the assumption that

$$|\Omega_{\text{eff}}| \ll \Gamma, \gamma, |\delta_r|, \nu. \tag{A18}$$

We denote the first integral in Eq. (A17) by $R_1(t)$ and the second integral by $R_2(t)$ such that

$$\mathbb{Q}\rho(t) = R_1(t) + R_2(t). \tag{A19}$$

Inserting in Eq. (A14) leads to

$$\begin{aligned}\mathbb{P}\dot{\rho}(t) = \mathbb{P}\mathcal{L}\mathbb{P}\rho(t) + \mathbb{P}\mathcal{L}_0 R_1(t) + \mathbb{P}\mathcal{L}_1 R_1(t) \\ + \mathbb{P}\mathcal{L}_0 R_2(t) + \mathbb{P}\mathcal{L}_1 R_2(t).\end{aligned} \tag{A20}$$

The term $\mathbb{P}\mathcal{L}_0 R_1(t) = 0$, and $\mathbb{P}\mathcal{L}_1 R_2(t)$ is a third-order term and can be neglected. Neglecting terms rotating with $\exp(\pm i\nu t)$ we get the master equation given by Eq. (6) with ac Stark shifts given by

$$H_S = s_- \sigma_k^+ \sigma_k^- + s_+ \sigma_k^- \sigma_k^+, \tag{A21}$$

where

$$s_\pm = \Omega_{\text{eff}}^2 \eta_1^2 \frac{(\delta_r \pm \nu)}{(\Gamma + \gamma)^2 + (\delta_r \pm \nu)^2}.$$

APPENDIX B: DERIVATION OF SPIN HAMILTONIAN

In the Mott-insulator regime, bosonic atoms trapped by a lattice potential with two motional states are described by the two-band Bose-Hubbard model

$$H_{\text{BH}} = H_0 + H_t. \tag{B1}$$

Here, the sum runs over the N sites k of the optical lattice. The unperturbed Hamiltonian H_0 is given by

$$H_0 = \sum_k \left(\frac{U_{01}}{2}\hat{n}_{k0}\hat{n}_{k1} + \sum_{x=0,1} \frac{U_{xx}}{2}\hat{n}_{kx}(\hat{n}_{kx} - 1) + \nu\hat{n}_{k1} \right),$$

where $U_{xx'}$ is the on-site repulsion of two atoms on lattice site k, where one atom is in motional state $|x\rangle$ and the other one is in $|x'\rangle$ with $x, x' = 0, 1$, respectively. The operator $\hat{n}_{kx} = |x\rangle\langle x|_k$ counts the number of atoms at lattice site k in the motional states $x = 0, 1$ and ν is the energy difference between ground and first-excited motional states. We assume the system to be prepared in the ground state $|0\rangle$. Due to the anharmonicity of the potential, we do not leave the subspace of $n = 0$ and $n = 1$ excitations.

The perturbative part of the Hamiltonian describes the tunneling between neighboring lattice sites and is given by

$$H_t = \sum_k t_0 c_{k,0}^\dagger c_{k+1,0} + t_1 c_{k,1}^\dagger c_{k+1,1} + \text{H.c.} \tag{B2}$$

Here, the operators c_{kx} with $x = 0, 1$ are bosonic destruction operators for atoms in the two motional states $|0\rangle$ and $|1\rangle$ at lattice site k. t_0 (t_1) are the tunneling amplitudes from state $|0\rangle$ ($|1\rangle$) at lattice site k to state $|0\rangle$ ($|1\rangle$) at $k + 1$.

As the on-site interaction $U_{xx'} \gg t_0, t_1$, tunneling between neighboring wells that leads to states with two atoms in one lattice well can be treated as a perturbation. For that, we consider two neighboring lattice sites k and $k + 1$ and write the effective Hamiltonian in the basis of eigenvectors of H_0, $|x_k, y_{k+1}\rangle$, where for example $|0_k, 1_{k+1}\rangle$ is the notation for the state with one particle in well k in state $|0\rangle$, and one particle in well $k + 1$ in state $|1\rangle$. In perturbation theory [25], the

second-order effective Hamiltonian can be evaluated in the following way:

$$\langle x_k, y_{k+1}|H_{\text{eff}}^{(3)}|x'_k, y'_{k+1}\rangle = \frac{1}{2}\sum_{\chi}\langle x_k, y_{k+1}|H_t|\chi\rangle\frac{1}{E'}\langle\chi|H_t|x'_k, y'_{k+1}\rangle, \quad \text{(B3)}$$

where

$$\frac{1}{E'} = \frac{1}{E_{xy} - E_\chi} + \frac{1}{E_{x'y'} - E_\chi},$$

and $|\chi\rangle$ are eigenstates of H_0 with two particles in one well (and no particle in the other one). $E_{xy} = \langle x_k, y_{k+1}|H_0|x_k, y_{k+1}\rangle$ and $E_\chi = \langle\chi|H_0|\chi\rangle$ are the unperturbed energies. Evaluating Eq. (B3) leads to the effective spin Hamiltonian $H_{\text{eff}}^{(3)}$ given by

$$H_{\text{eff}}^{(3)} = H_{\text{spin}} + B_z\sum_k |1\rangle\langle 1|_k, \quad \text{(B4)}$$

with

$$H_{\text{spin}} = \sum_k \alpha_1\left(\sigma_k^x\sigma_{k+1}^x + \sigma_k^y\sigma_{k+1}^y\right) + \alpha_2\sigma_k^z\sigma_{k+1}^z. \quad \text{(B5)}$$

Here,

$$\alpha_1 = -\frac{4t_0t_1}{U_{01}}, \quad \alpha_2 = 2\left(\frac{t_0^2 + t_1^2}{U_{01}} - \frac{t_0^2}{U_{00}} - \frac{t_1^2}{U_{11}}\right),$$

and B_z, the magnetic field in z direction, is

$$B_z = \frac{t_0^2}{U_{00}} - \frac{t_1^2}{U_{11}}.$$

Thus, we have derived an effective XXZ-spin Hamiltonian with a magnetic field in the z direction.

APPENDIX C: CONDITION FOR DISCONTINUOUS BEHAVIOR

Here, we first derive a general condition for the discontinuous behavior in the steady state at a degeneracy point of a large class of spin Hamiltonians. Next, we focus on more specific Hamiltonians. We study the steady state of flip-invariant Hamiltonians outside the degeneracy point and, starting with the general condition for finding discontinuities in the steady state, we derive a more precise condition for flip-invariant Hamiltonians.

1. General condition for discontinuities in steady state

Here, we derive a general condition for discontinuous behavior in the steady state at the degeneracy point $x = x_0$ of a general Hamiltonian H, where $H = H(x)$ is an analytic function of x. We consider a system described by the master equation

$$\dot\rho(t) = (\mathcal{L}_0 + \mathcal{L}_1)\rho(t), \quad \text{(C1)}$$

where the Hamiltonian part of the Liouvillian is given by $\mathcal{L}_0(x) = \mathcal{L}_0 = -i[H(x),\cdot]$ and depends on a parameter x, and the local decay Liouvillian is

$$\mathcal{L}_1\rho(t) = \sum_k \gamma_k[2\sigma_k^-\rho(t)\sigma_k^+ - \{\sigma_k^+\sigma_k^-, \rho(t)\}_+]. \quad \text{(C2)}$$

First, we want to describe the system outside the degeneracy point, i.e., for $x \neq x_0$. We assume that in the vicinity of x_0, the Hamiltonian is nondegenerate (for $x \neq x_0$) and that the dissipation is weak. The steady state $\rho_{ss}(x)$ defined by $(\mathcal{L}_0(x) + \mathcal{L}_1)\rho_{ss}(x) = 0$ is, in the limit $\gamma \to 0$, given by

$$\mathrm{P}^D(x)\mathcal{L}_1\mathrm{P}^D(x)\rho_{ss} = 0, \quad \text{(C3)}$$

where $\mathrm{P}^D(x)$ is the projector onto the kernel($\mathcal{L}_0$). As the kernel of $\mathcal{L}_0$ is spanned by the eigenprojectors $|\lambda_i(x)\rangle\langle\lambda_i(x)|$ of H we have for arbitrary A

$$\mathrm{P}^D A = \sum_i |\lambda_i(x)\rangle\langle\lambda_i(x)|A|\lambda_i(x)\rangle\langle\lambda_i(x)|, \quad \text{(C4)}$$

where $|\lambda_i(x)\rangle$ are eigenstates of the Hamiltonian $H(x)$ which is assumed to be nondegenerate.

Now, let us consider the case that at $x = x_0$, the Hamiltonian has a degeneracy point at which two or more eigenvalues cross. At this degeneracy point, we expect a discontinuous behavior of the steady state that leads to the peaks we observe in our numerical simulation (see Figs. 6–9). At $x = x_0$ the projector onto the kernel of $\mathcal{L}_0$ has to be extended. It now also projects onto coherences between eigenstates of H: $|\lambda_1\rangle$,$|\lambda_2\rangle$ which are eigenvectors to the degenerate eigenvalues $\lambda_1 = \lambda_2$. Therefore the projector on the coherences reads

$$\mathrm{P}^\Delta A = |\lambda_1\rangle\langle\lambda_1|A|\lambda_2\rangle\langle\lambda_2| + \text{H.c.} \quad \text{(C5)}$$

It is convenient to define a continuous extension of the projector P^D at $x = x_0$, which reads

$$\mathrm{P}^D(x_0) = \lim_{x\to x_0}\mathrm{P}^D(x). \quad \text{(C6)}$$

Thus, at $x = x_0$, the full projector onto the kernel of $\mathcal{L}_0$ reads $\mathrm{P}^D(x_0) + P^\Delta$. Now the condition for the steady state $\rho_{ss}(x = x_0)$ at the degeneracy point is given by

$$[\mathrm{P}^D(x_0) + \mathrm{P}^\Delta]\mathcal{L}_1[\mathrm{P}^D(x_0) + \mathrm{P}^\Delta]\rho_{ss}(x_0) = 0. \quad \text{(C7)}$$

We want to find a sufficient condition for the steady state to change discontinuously. This means that

$$\rho_{ss}(x_0) - \lim_{x\to x_0}\rho_{ss}(x) \neq 0, \quad \text{(C8)}$$

where $\lim_{x\to x_0}\rho_{ss}(x)$ is the continuous extension of $\rho_{ss}(x)\ \forall\ x \neq x_0$ to $x = x_0$.

A discontinuity in the steady state as described by Eq. (C8) can occur only if

$$[\mathrm{P}^D(x_0) + \mathrm{P}^\Delta]\mathcal{L}_1[\mathrm{P}^D(x_0) + \mathrm{P}^\Delta]\lim_{x\to x_0}\rho_{ss}(x) \neq 0 \quad \text{(C9)}$$

holds, since otherwise the continuous extension $\lim_{x\to x_0}\rho_{ss}(x)$ would be a steady state as well. The last part of Eq. (C9) can be simplified using

$$[\mathrm{P}^D(x_0) + \mathrm{P}^\Delta]\lim_{x\to x_0}\rho_{ss}(x) = \lim_{x\to x_0}\rho_{ss}(x),$$

which holds since $\lim_{x\to x_0}\rho_{ss}(x)$ is per definition in the space onto which $\mathrm{P}^D(x_0)$ projects and P^Δ is orthogonal to that space. By Eq. (C3) we then see that Eq. (C9) reduces to the condition

$$\mathrm{P}^\Delta\mathcal{L}_1\lim_{x\to x_0}\rho_{ss}(x) \neq 0. \quad \text{(C10)}$$

If this condition is fulfilled, then $\rho_{ss}(x_0) - \lim_{x\to x_0}\rho_{ss}(x) \neq 0$ which means that the steady state shows discontinuous behavior at the degeneracy point $x = x_0$.

2. Condition for discontinuous behavior for Ising Hamiltonians

Here, we want to get a better insight into how the condition given by Eq. (C10) relates to the peaks observed in our numerical simulation. In the following, we will apply it to the Ising model in a transverse magnetic field. In the numerical simulation (see Fig. 8) for the Ising Hamiltonian with periodic boundary conditions under collective dissipation described by Eq. (24), we restrict our consideration to a specific subspace with eigenvalue 1 for the translation operator T and the reflection operator R: $T = R = 1$. First, we want to prove that if the steady state is unique, then it is the fully mixed state outside the degeneracy points as indicated by our numerical simulation. Then we show that, starting from the condition given by Eq. (C10), specialization to the Ising model allows us to derive a more precise condition for finding a discontinuity in the steady state at the degeneracy points.

First, we show that $\mathbb{1}$ satisfies $(\mathcal{L}_0 + \mathcal{L}_1)\mathbb{1} = 0$ outside the degeneracy point $x \neq x_0$. Therefore, for systems with a unique steady state, it is given by the fully mixed state for $x \neq x_0$ in the limit $\gamma \to 0$. The Hamiltonian given by Eq. (21) is assumed to be nondegenerate for $x \neq x_0$ and invariant under the spin-flip operator $F = \sigma_x^{\otimes N}$, i.e., $FHF^\dagger = H$. Thus, we want to show that, for $x \neq x_0$,

$$\mathrm{P}^D \mathcal{L}_1 \mathbb{1} = 0, \tag{C11}$$

where P^D is given by Eq. (C4). Then,

$$\mathrm{P}^D \mathcal{L}_1(\mathbb{1}) = 2\gamma(J^- J^+ - J^+ J^-) \propto \gamma J^z. \tag{C12}$$

Therefore, Eq. (C11) reads

$$\mathrm{P}^D \mathcal{L}_1(\mathbb{1}) = \mathrm{P}^D J^z = \sum_i |\lambda_i\rangle\langle\lambda_i|J^z|\lambda_i\rangle\langle\lambda_i| = 0. \tag{C13}$$

If we can show that Eq. (C13),

$$\langle\lambda_i|J^z|\lambda_i\rangle = 0 \;\forall\, i, \tag{C14}$$

then we have shown that the fully mixed state is a steady state of our system outside the degeneracy points of the Hamiltonian.

As the Hamiltonian is nondegenerate and invariant under the flip-operator F, the eigenvectors of H are eigenvectors of F: $F|\lambda_i\rangle = \alpha_i|\lambda_i\rangle$. Let $|\alpha\rangle$ denote an arbitrary eigenvector of H with F eigenvalue α. Since the spectrum of F is $\{\pm 1\}$, we have $|\alpha\rangle = \alpha^2|\alpha\rangle = \alpha F|\alpha\rangle$. Moreover, the flip F changes the sign of J^z, i.e, J^z and F anticommute: $\{F, J^z\}^+ = 0$. Therefore, we can write Eq. (C14) as

$$\begin{aligned}\langle\alpha|J^z|\alpha\rangle &= \alpha\langle\alpha|J^z F|\alpha\rangle \\ &= -\alpha\langle\alpha|FJ^z|\alpha\rangle = -\langle\alpha|J^z|\alpha\rangle,\end{aligned} \tag{C15}$$

where we have used $\alpha^2 = 1$. It follows that

$$\langle\alpha|J^z|\alpha\rangle = 0. \tag{C16}$$

Consequently, $\mathrm{P}^D\mathcal{L}_1(\mathbb{1}) = 0$ and we have shown that in the limit of weak dissipation, the steady state, if it is unique, is the fully mixed state. For the Ising model with up to eight atoms and collective dissipation, we know from our numerics that the steady state is unique.

To see that the steady state shows discontinuous behavior at the degeneracy point $x = x_0$, we need now only to show that the fully mixed state is not the steady state of the system. Thus, we need to show that

$$\mathrm{P}^\Delta \mathcal{L}_1(\mathbb{1}) = \mathrm{P}^\Delta J^z = \sum_{i,j,i\neq j}{}' |\lambda_i\rangle\langle\lambda_i|J^z|\lambda_j\rangle\langle\lambda_j| \neq 0, \tag{C17}$$

where P^Δ is given by Eq. (C5) and $\sum'$ sums over the labels of degenerate eigenvalues. Since the eigenvectors are orthogonal, Eq. (C17) holds if $\exists\, i \neq j$ such that

$$\langle\lambda_i|J^z|\lambda_j\rangle \neq 0. \tag{C18}$$

Therefore, Eq. (C18) gives a condition for finding discontinuous behavior of the steady state of the Ising model in a transverse field under collective dissipation. Note that this derivation can be easily extended to all nondegenerate Hamiltonians that are flip invariant.

[1] S. Sachdev, *Quantum Phase Transitions* (Cambridge University Press, Cambridge, MA, 1999).
[2] I. Bloch, Nat. Phys. **1**, 23 (2005).
[3] W. H. Zurek, Rev. Mod. Phys. **75**, 715 (2003).
[4] B. Baumgartner and H. Narnhofer, Rev. Math. Phys. **24**, 1250001 (2012).
[5] A. Beige, S. Bose, D. Braun, S. F. Huelga, P. L. Knight, M. B. Plenio, and V. Vedral, J. Mod. Opt. **47**, 2583 (2000).
[6] F. Benatti, R. Floreanini, and M. Piani, Phys. Rev. Lett. **91**, 070402 (2003).
[7] B. Kraus, H. P. Büchler, S. Diehl, A. Kantian, A. Micheli, and P. Zoller, Phys. Rev. A **78**, 042307 (2008).
[8] C. A. Muschik, E. S. Polzik, and J. I. Cirac, Phys. Rev. A **83**, 052312 (2011).
[9] F. Verstraete, M. M. Wolf, and J. I. Cirac, Nat. Phys. **5**, 633 (2009).
[10] K. G. H. Vollbrecht, C. A. Muschik, and J. I. Cirac, Phys. Rev. Lett. **107**, 120502 (2011).
[11] H. J. Carmichael, J. Phys. B **13**, 3551 (1980).
[12] F. Dimer, B. Estienne, A. S. Parkins, and H. J. Carmichael, Phys. Rev. A **75**, 013804 (2007).
[13] S. Morrison and A. S. Parkins, Phys. Rev. A **77**, 043810 (2008).
[14] S. Diehl, A. Micheli, A. Kantian, B. Kraus, H. P. Buchler, and P. Zoller, Nat. Phys. **4**, 878 (2008).
[15] J. Eisert and T. Prosen, arXiv:1012.5013.
[16] M. Müller, S. Diehl, G. Pupillo, and P. Zoller, Adv. At. Mol. Opt. Phys. **61**, 1 (2012).
[17] M. Lewenstein, A. Sanpera, and V. Ahufinger, *Ultracold Atoms in Optical Lattices* (Oxford University Press, Oxford, UK, 2012).
[18] J. J. García-Ripoll and J. I. Cirac, New J. Phys. **5**, 76 (2003).
[19] J. Simon, W. S. Bakr, R. Ma, M. E. Tai, P. M. Preiss, and M. Greiner, Nature (London) **472**, 307 (2011).
[20] D. Jaksch and P. Zoller, Ann. Phys. (NY) **315**, 52 (2005).
[21] C. Navarrete-Benlloch, I. de Vega, D. Porras, and J. I. Cirac, New J. Phys. **13**, 023024 (2011).
[22] $|0\rangle_j$ denotes the localized Wannier function at site j, where 0 is the band index.

[23] E. Charron, E. Tiesinga, F. Mies, and C. Williams, in *Quantum Communication, Computing, and Measurement 3*, edited by P. Tombesi and O. Hirota (Kluwer, New York, 2002), pp. 227–230.
[24] For details see Eq. (20).
[25] C. Cohen-Tannoudji, J. Dupont-Roc, and G. Grynberg, *Atom-Photon Interactions* (Wiley Intersciences, New York, 1992).
[26] I. Marzoli, J. I. Cirac, R. Blatt, and P. Zoller, Phys. Rev. A **49**, 2771 (1994).
[27] Note that $\sin(k_b x_k) \approx \eta_b(c_k + c_k^\dagger)$ where c_k are bosonic operators that describe the harmonic oscillator states of the trapping potential. As explained before, we work in the truncated subspace of $|0\rangle$ and $|1\rangle$ due to the anharmonicity of the trap and the cooling to the ground state such that the $\eta_b(c_k + c_k^\dagger) = \eta_b(\sigma_k^- + \sigma_k^+)$.
[28] D. Jaksch, C. Bruder, J. I. Cirac, C. W. Gardiner, and P. Zoller, Phys. Rev. Lett. **81**, 3108 (1998).
[29] $U_{xx'}$ is the on-site repulsion of two atoms on lattice site k, where one atom is in motional state $|x\rangle$ and the other one in $|x'\rangle$ with $x, x' = 0, 1$, respectively.
[30] P. Werner, K. Völker, M. Troyer, and S. Chakravarty, Phys. Rev. Lett. **94**, 047201 (2005).
[31] M. Žnidarič, Phys. Rev. E **83**, 011108 (2011).
[32] Here we use that if $H(x)$ is a holomorphic function of x (we are typically concerned with linear dependence on x only) the eigenvectors of $H(x)$ can be chosen as holomorphic (and thus continuous) functions of $x \in \mathbb{R}$ [38]. Then, $\lim_{x\to x_0} P^D(x_0)$ is well defined and we can define P^Δ as the difference of the projector on the kernel of $\mathcal{L}_0(x_0)$ and $\lim_{x\to x_0} P^D(x_0)$.
[33] P. Zanardi and N. Paunković, Phys. Rev. E **74**, 031123 (2006).
[34] A. Uhlmann, Rep. Math. Phys. **9**, 273 (1976).
[35] If initialized in this subspace (e.g., by optically pumping it to the fully polarized states $|0\rangle^{\otimes N}$), the system will remain there since both $\mathcal{L}_0$ and $\mathcal{L}_1$ respect these symmetries.
[36] P. Pfeuty, Ann. Phys. (NY) **57**, 79 (1970).
[37] A. Messiah, *Quantenmechanik Band 2* (de Gruyter, Berlin, 1985).
[38] T. Kato, *Perturbation Theory for Linear Operators* (Springer, Berlin, Heidelberg, 1995).